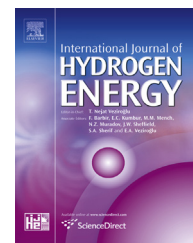


Available online at [www.sciencedirect.com](http://www.sciencedirect.com)

ScienceDirect

journal homepage: [www.elsevier.com/locate/hydro](http://www.elsevier.com/locate/hydro)

# Impedance model for diagnosis of water management in fuel cells using artificial neural networks methodology

Slimane Laribi <sup>a,b,\*</sup>, Khaled Mammar <sup>a</sup>, Messaoud Hamouda <sup>b</sup>,  
Yousef Sahli <sup>b,c</sup>

<sup>a</sup> Department of Electrical and Computer Engineering, University of Tahri Mohamed Béchar, Bp 417, Algeria

<sup>b</sup> Unité de Recherche en Energies Renouvelables en Milieu Saharien, URERMS, Centre de Développement des Energies Renouvelables, CDER, 01000, Adrar, Algeria

<sup>c</sup> Department of Mechanical, Faculty of Technology, University Hadj Lakhder, Batna, Algeria

## ARTICLE INFO

### Article history:

Received 23 February 2016

Received in revised form

16 June 2016

Accepted 13 July 2016

Available online xxx

### Keywords:

Water management

Electrochemical impedance spectroscopy

PEMFC

Impedance model

Flooding

Drying

## ABSTRACT

The objective of this work is to define and to implement a simple method to assess the impacts of relative humidity and operating time on the fuel cell impedance. The method is based on the physical model of Randles with CPE and a mathematical tool for identifying various parameters based on the least squares method. The objective of the theoretical model development is the model implementation of the control system and water management of predictive diagnostics. Artificial neural networks are used to create the optimum impedance model. The model is applied for the identification of all resistors (internal resistors measured at high frequency, biasing resistors measured at high frequency) which are characterized by a high sensitivity for both cases, the flooding or drying of the cell heart (membrane and electrodes). This model is able to easily generate Nyquist diagram for any condition of relative humidity and operating time, it helped define the stack hydration status. Based on the obtained results, the model demonstrated a best flexible response, accurate and fast. The developed model can be integrated into a water management control system in PEM fuel cells.

© 2016 Hydrogen Energy Publications LLC. Published by Elsevier Ltd. All rights reserved.

## Introduction

Fuel cell is the device of chemical energy conversion into electrical energy without harmful gas emissions. Compared to the other renewable energy technology types, the fuel cell has a stable power generation and a high-efficiency compared to internal combustion engines and a total independence from fossil resource use. Proton Exchange Membrane (PEM) is a fuel

cell type that works in low temperature (70–120 °C), it is characterized by a high efficiency and one of the promising technologies in future [1–7].

PEMFC converts the fuel chemical energy into electrical energy. The typical outline PEMFC is illustrated in Fig. 1 [2]. In the first cell side, which is named the anode, the fuel is feed under certain pressure. The used fuel this model is the pure hydrogen, although other gas compositions can be used in this process.

\* Corresponding author. Department of Electrical and Computer Engineering, University of Tahri Mohamed Béchar, Bp 417, Algeria.

E-mail address: [laribi\\_86@yahoo.fr](mailto:laribi_86@yahoo.fr) (S. Laribi).

<http://dx.doi.org/10.1016/j.ijhydene.2016.07.099>

0360-3199/© 2016 Hydrogen Energy Publications LLC. Published by Elsevier Ltd. All rights reserved.

## Nomenclature

$C_{dl}$	Double layer capacitance, F
$C$	Oxygen concentration in cathode active layer, mol m <sup>-3</sup>
$\delta$	Diffusion layer width, m
$D$	Diffusion coefficient, m <sup>2</sup> s <sup>-1</sup>
$F$	Faraday constant, As mol <sup>-1</sup>
$N$	Number of electrons
$R$	Perfect gas constant, J mol <sup>-1</sup> K <sup>-1</sup>
$R_d$	Electrical resistance, $\Omega$
$R_m$	Ohmic resistance of the electrolyte, $\Omega$
$R_p$	Electrical resistance, $\Omega$
$R_{int}$	Internal resistors measured at high frequency, $\Omega$
$R_{pol}$	Biassing resistor measured at low frequency, $\Omega$
$f_{max}$	Arc-summit frequency, Hz
$I_{max}$	Arc-summit imaginary, $\Omega$
$Q$	Parameter of the CPE, S s <sup><math>\alpha</math></sup>
RH	Relative humidity, %
$S$	Active area, m <sup>2</sup>
$T$	Temperature, K
$Z$	Fuel cell's impedance, $\Omega$
$Z_{CPE}$	CPE impedance
$Z_w$	Warburg impedance, $\Omega$
$\tau_d$	Time constant of diffusion, s
$\alpha$	Power of the CPE
$\omega$	Pulsation, rad s <sup>-1</sup>
$j$	Imaginary number

In order to get an electric current out of this reaction, the hydrogen dissociation into protons and electrons at the anode which is represented by Eq. (1), and the oxygen reduction at the cathode Eq. (2) these two electrodes are separated by a membrane, which is conducting the protons from the anode to the cathode.



The proton products pass through the solid polymer membrane and the electrons are forced to pass through an external circuit, producing electricity, this process is shown in Fig. 1.

The PEM successful operation is linked to a water management problem in the gas feed channels.

The proton conductive membrane must be saturated with water, which is essential to ensure a good ionic conductivity [3]. For this reason, the membrane continuous drying led directly to a stack mandatory arrest, it better works after a while of use, because the water is produced in the cathode (hydration of the membrane), after this commissioning time, the excess water must be continuously removed to avoid the flooding and the waterlogging of the cell (gas transport blockage in the electrodes). Consequently, water management is one of the most critical parameter of PEM fuel cell design [4]. Several scientific research are released in this domain. Thomas G  n  v   et al. [5] have analyzed flooding diagnosis based on time-constant spectrum. The proposed method is based on the fuel cell voltage response; a deconvolution procedure is used to extract the equivalent time-constant spectrum. Fouquet et al. [4] have proposed and examined the monitoring of flooding and drying of PEM fuel cell, they are using a model-based approach coupled with impedance measurements. The classical Randles cell was extended by changing the standard plane capacitor into a constant phase element (CPE), in order to improve the fit quality. Mammar et al. [6] have developed a suitable PEMFC impedance model, which can be used for PEM fuel cell diagnosis. They are using a novel optimization method based on the factorial design methodology. This procedure is applied for the electrochemical impedance parametric analysis for PEMFC impedance behavior analysis in the flooding and drying cases. Dotelli et al. [7] have presented an experimental analysis for testing the ohmic resistance in the membrane drying case, and method sensitivity discussing in the membrane dehydration case. Also, they are discussed, the

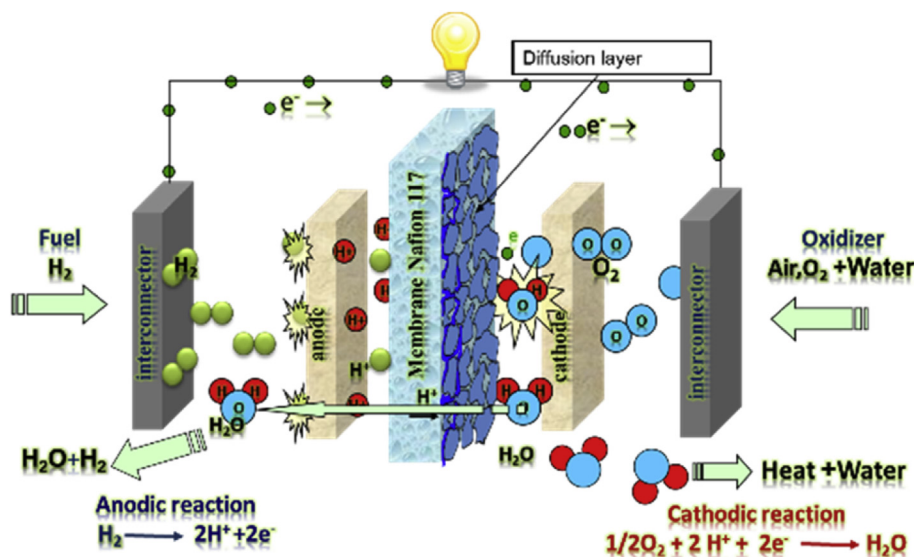


Fig. 1 – Basic fuel cell operation.

possibility to effectively detect the flooding conditions by exploiting only the available ripple response and the approach testing for the diagnosis. Murugesan et al. [8] have studied the effect of water management dynamics over the system behavior. They are showing that the model responses fit well with the experimental results. The presented model by this author is capable to predict the dynamic and transient response of stack voltage/power under a sudden change in load current. The developed model can be used to optimize the stack performance in terms of water management, which facilitates in developing an optimized structural design of the fuel cell stack system.

Artificial Neural Network technology is a modeling modern technique, which is often used in the fuel cell model developments [9–12]. Arriagada et al. [12] have developed a SOFC model based on an artificial neural network for studied the fuel cell performance. Hatti et al. [11] have presented a dynamic neural network controller model that use the Quasi-Newton–Levenberg–Marquardt control algorithm.

The objective of this work is to define and implement a simple method to assess the impacts of relative humidity and operating time on the impedance. The method is based on the physical model of Randles changes (CPE) and a mathematical tool for identifying various parameters based on the least squares method. The objective of the theoretical model development is the model implementation of the control system and water management of predictive diagnostics. Artificial neural networks are used to create the optimum impedance model. The model is applied for the identification of all resistors (internal resistors measured at high frequency, biasing resistors measured at high frequency) which are characterized by a high sensitivity for both cases, the flooding or drying of the cell heart (membrane and electrodes).

## PEM fuel cell impedance model

When there is no mass transport limitation, the redox reaction is simply represented by an equivalent electrical circuit of parallel RC cells. However, when there are considerable variations of the interfacial concentrations on electrodes, the Randles cell is a common and practical way of electrochemical cell modeling by an equivalent circuit [13–17]. It consists of four elements: two resistors,  $R_m$  is the electrolyte ohmic resistance and  $R_p$  is the polarization resistance, one plane capacitor,  $C_{dl}$  which represent the double layer capacitance at the electrode/electrolyte interface; and the impedance of diffusion called Warburg impedance.

The diffusion impedance general expression for a finite length diffusion layer  $Z_w$  is given by [4,6,18]:

$$Z_w(j\omega) = \frac{RT}{n^2 F^2 S \sqrt{j\omega}} \frac{\tanh \sqrt{(j\omega)/D} \delta^2}{C \sqrt{D}} \quad (3)$$

The relation (3) can be re-written as:

$$Z_w(j\omega) = \frac{RT}{n^2 F^2 S \sqrt{j\omega}} \frac{1}{C} \frac{1}{D} \delta \frac{\tanh \sqrt{(j\omega)(\delta^2/D)}}{C \sqrt{\delta^2/D}} \quad (4)$$

Which leads to the definition of two parameters, a time constant:

$$\tau_d = \frac{\delta^2}{D} \quad (5)$$

In addition, the resistance:

$$R_d = \frac{RT\delta}{n^2 F^2 S C D} \quad (6)$$

This leads to the final expression of the concentration diffusion impedance:

$$Z_w(j\omega) = R_d \frac{\tanh \sqrt{(j\omega)(\delta^2/D)}}{C \sqrt{\delta^2/D}} \quad (7)$$

The fuel cell total impedance is composed by two impedances, one impedance for each electrode (anode and cathode), which are in series with the internal resistance  $R_m$ . We assume that the rate limiting reaction is the oxygen reduction is directly related to the cathode, and we neglect the anode impedance contribution to the cell impedance. Thus, the retained fuel cell equivalent circuit model is represented by Fig. 2, and the overall impedance is:

$$Z(j\omega) = R_m + \frac{1}{j\omega C_d + (1/(R_p + Z_w))} \quad (8)$$

In Fig. 3, the Randles cell fitting to the experimental data, but not entirely satisfactory. The bulk of the problem comes from the high-frequency part of the model, for which the

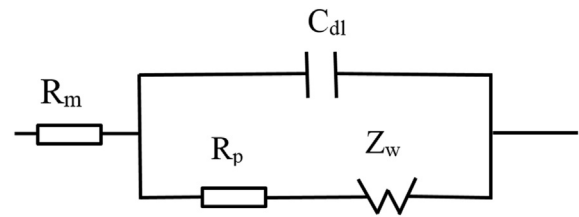


Fig. 2 – Randles cell.

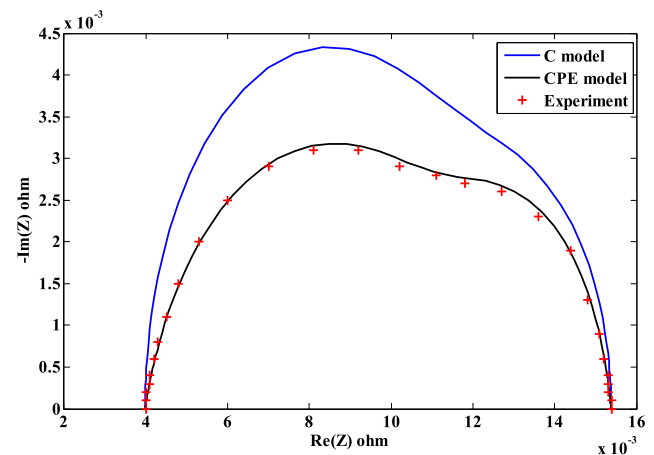


Fig. 3 – Comparison between experimental impedance data and the both Randles models (with  $C_{dl}$  and with CPE).

Randles cell predicts a semicircle centred on the x-axis, experimentally, data clearly show a depressed semicircle (i.e. centered below the x-axis). As a side effect, the model misplaces the transition between the two semicircles. These depressed semicircles are dealt with by the standard plane capacitor change of the Randles circuit by a constant phase element (CPE) [16]. As indicated in Fig. 4, the standard plane capacitor exhibits the first-order behavior, CPE impedance is defined by Refs. [19–22]:

$$Z_{CPE}(j\omega) = \frac{1}{Q(j\omega)^\alpha} \quad (9)$$

With a value of  $\alpha$  usually ranging between 0.5 and 1. Thus, the impedance of the equivalent circuit is now:

$$Z_T(j\omega) = R_m + \frac{1}{Q(j\omega)^\alpha + (1/(R_p + Z_w))} \quad (10)$$

### PEMFC dynamic characterization by an artificial neural network model

Neural networks are now an actual tool of resolution several problems which cannot be resolved by conventional methods. The neural network method principle is based on the function approximations. In this study, we used a neural network of type feed-forward with a supervised training to build a network of four main construction steps:

- RNA block construction.
- Data acquisition (Learning base).
- Classification of various defects.
- Network test.

The neural network is composed of three layers principal, namely: An input layer, a hidden layer and an output layer. Each neuron is connected to all neurons of the next layer.

The used transfer function in the hidden layer is a sigmoid function; it is given by the following [23,24]:

$$f(u) = \frac{1}{1 + e^{-(d \cdot u)}} \quad (11)$$

With  $d$  is the curve slope. The hidden layer input is given by the following equation [23,24]:

$$u = \sum_{j=1}^n (w_{ij}x_i + b_i) \quad (12)$$

Where  $x_i$  is the input signal,  $w_{ij}$  is the weight on the connection between neurons  $i$ th and  $j$ th in the hidden layer and  $b_i$  is the bias.

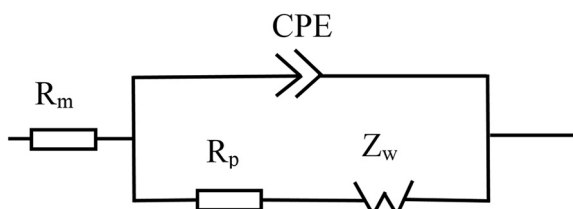


Fig. 4 – Equivalent circuit proposed by Fouquet et al. [4].

When the output layer function is linear, the network model equation is given by the following equation [23,24]:

$$y_k u = \sum_{j=1}^N (w_{kj}^0 u_j + b_k) = \sum_{j=1}^N w_{kj}^0 f \left( \sum_{i=1}^N (w_{ji} x_i + b_i) \right) \quad (13)$$

Where  $y_k$ , is the output signal from  $k$ th output neuron,  $w_{ki}^0$  is the weight of  $i$ th output  $u_i$  to the  $k$ th neuron in the output layer.

In this work, the ANN bias values and the weight are updated according to the dynamic gradient descent algorithm [25].

Fig. 5 represented the neural network model architecture used in the present work. The input layer part of Neural network is composed of three input neurons, the first part is linked at the humidity rate, the second part is linked at the operation time, the third part is linked at the frequency. The hidden layer part is composed of two under hidden layers with twenty neurons of the first and ten neurons for the second; the last part (output layer) is composed of two neurons of output. (Re (Z), Im (Z)).

For PEMFC parameter simulation, we completed the development of a MATLAB code based on the model already presented by using Neural networks toolbox. The hyperbolic tangent sigmoid transfer function (“tansig”) is used for estimations of the parameters in the hidden layer part and the linear transfer function (“purelin”) is applied to the output layer.

The mean square error is represented in Fig. 6. After 100,000 iterations, the mean square error of ANN reaches a very low value that equal  $1.5977 \times 10^{-18}$ .

Network learning error is shown in Fig. 7, where the error is almost zero learning (about  $10^{-12}$ ); this proves the ANN learning reliability.

### Model test and validation

To establish the learning of our neural network, the database selection is mandatory. The model learning parameter values are given by Table 1 for four impedance spectra for both flooding and drying cases of the fuel cell membrane [4,6]. The identifying Randles model parameters with CPE is made by the least square method. Once the neural network-training phase is complete, we go later in the testing phase of impedance spectrum quality estimates, for us the proceeds we presented another database, which is totally different to the

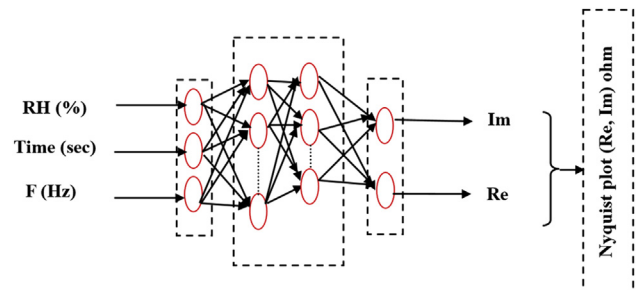


Fig. 5 – PEMFC neural networks model.



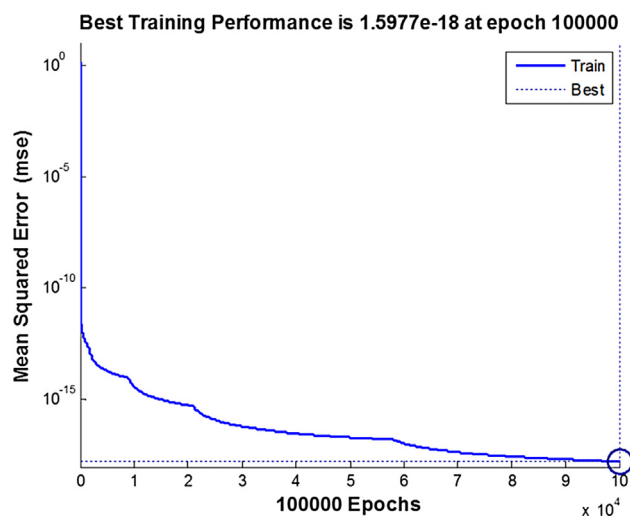


Fig. 6 – Training mean squared errors for NNT impedance model.

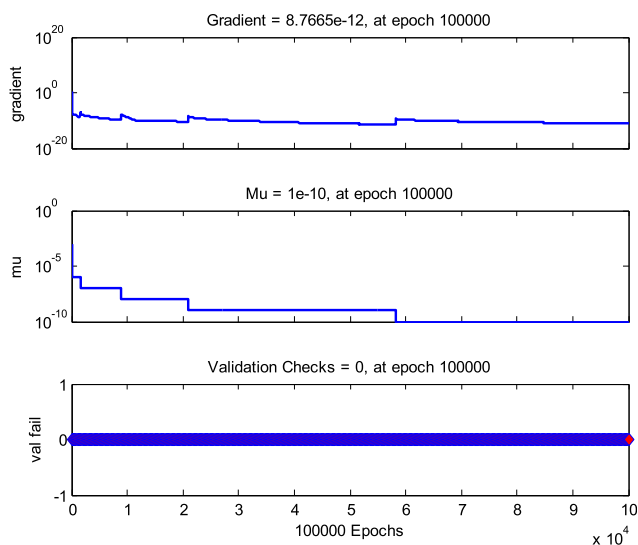


Fig. 7 – Output errors of the ANN impedance model during learning.

training base for the verification and validation of the procedure used.

We have taken the necessary input parameters for our model of the first test of Fig. 8 presented by Fouquet et al. [4], where the time is 500 s, RH = 100% and the Frequencies ranging from 0.1 Hz to 1 kHz, the third test of Fig. 8 [4], where

Table 1 – Model parameters and cell voltage during the flooding and drying [4,6].

Time (s)	RH (%)	$R_m$	$Q$	$R_p$	$R_d$	$\tau_d$	$U$
500	15	0.00512	0.952	0.0099	0.0051	0.1155	4.06
3700	15	0.0088	0.62	0.013	0.0101	0.1835	3.35
500	100	0.00398	1.109	0.008	0.0034	0.0872	4.18
3700	100	0.00416	0.936	0.0163	0.0312	0.0947	3.3

the time is 1000 s, RH = 100% and the Frequencies ranging from 0.1 Hz to 1 kHz, the fifth test of Fig. 8 [4], where the time is 1600 s, RH = 100% and the Frequencies ranging from 0.1 Hz to 1 kHz and the twelve test of Fig. 8 [4], where the time is 3600 s, RH = 100% and the Frequencies ranging from 0.1 Hz to 1 kHz, these all test represents a membrane flooding case.

For testing the membrane drying case, we have taken the test necessary input parameters from Fig. 10 presented by Fouquet et al. [4], where the time is neighbor 180 s, RH = 15% and the Frequencies ranging from 0.1 Hz to 1 kHz.

Then we compared our results with these experimental tests N° 1 and N° 5 of Fig. 9 presented by Fouquet et al. [4] for the flooding case and the test N° 1 of Fig. 11 for the membrane drying case presented by the same authors. The comparison between the experimental and numerical results indicates that the procedure used is reliable (Fig. 8).

## Simulation results and discussion of the impedance response

The progressive behavior simulation of impedance is realized by the time varies from (500 s–2500 s) at dehydrating conditions RH = 10% (dry gas). The spectra Nyquist plots from PEMFC fuel cells are characterized by the dehydration effect. Fig. 9a, they show a right lateral shift by the membrane resistance increase  $R_{int}$ . Under high load conditions, the fuel cell current density increasing, which provokes an increasing of water production at the cathode, this can lead to the flooding case.

The fuel cell drying effect is also be seen in the Bode diagram. Fig. 9b, this diagram shows an increase of the fuel cell impedance as a function of the time throughout the frequency range and an increase (less capacitive) in the phase angle at the high frequency medium (Fig. 9c).

The progressive behavior simulation of impedance is realized by a time varying from (500 s–2500 s) under flooding conditions RH = 100%. The spectra Nyquist plot from PEMFCs characterized the hydration effect (Fig. 10a), in this case, the large variations are absent in the high-frequency arcs. This behavior is induced by the increasing of the fuel cell current density, which provokes an increasing of water production at the cathode; this can lead to the flooding case. The initial stage of flooding is characterized by a slow decrease in the fuel cell output voltage, also, the liquid water begins to accumulate in the channels and constrict the gas flow, thus increasing the diffusion which is related to equivalent circuit parameter  $R_d$  and time constant  $\tau_d$ .

The fuel cell flooding effect is also be presented by the Bode diagram of Fig. 10b. We note, a impedance increase at low frequency accompanied by a decrease in the phase angle (more capacitive) (Fig. 10c).

The impedance phase behavior is simulated with a relative humidity variable (RH %) for a time of 500 s and 2500 s. The spectra Nyquist plot of PEMFCs characterizes the hydration effect (Figs. 11 and 12).

Figs. 11 and 12 show that the resistance measured value at a high stack frequency  $R_{int}$  increases with time, when the cathode relative humidity decreases from 100% at 10%. The resistance measured at low stack frequency  $R_{pol}$  gradually

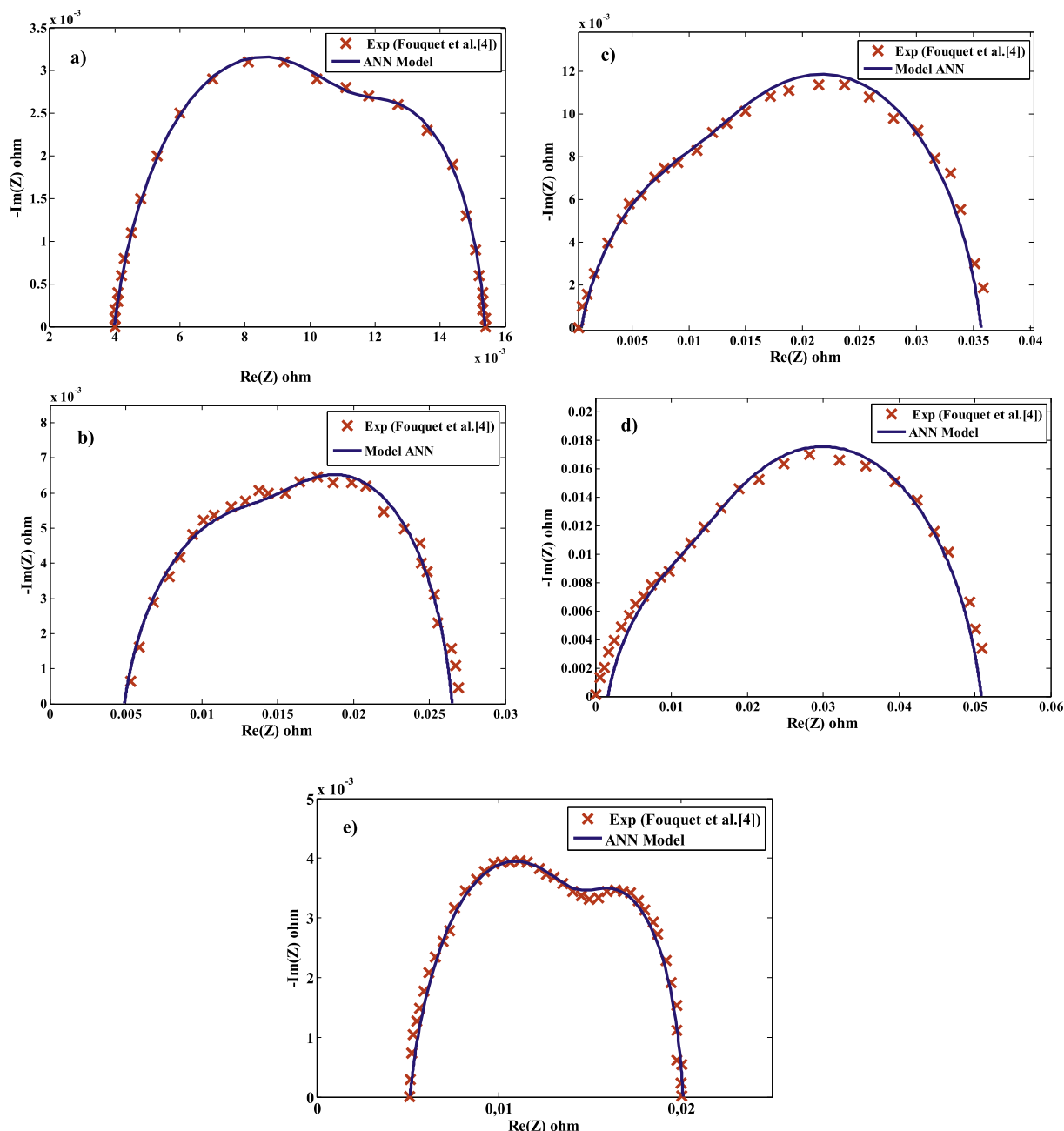


Fig. 8 – PEMFC model validation. a)–d) Flooded case, e) drying case.

increases, according to the time when the cathode relative humidity is increasing.

To make a diagnostic of flooding or drying, we conduct simulations of the impedance progressive behavior with a time of 500 s–3700 s, and a relative humidity of 10%–150%, then, we use the five criteria of the impedance (the internal resistor measured at high frequency, the biasing resistor measured at low frequency, the arc-summit frequency, the arc-summit imaginary and the Nyquist diagram area).

Fig. 13, show that the resistance measured value of a high stack frequency  $R_{int}$  increases with time when the cathode relative humidity decreases from 150% to 10%, because the stack membrane conductivity is directly related to its water

content. When relative humidity increases, the water content in membrane increases, consequently the membrane conductivity increases and the stack internal resistance will decrease.

The resistance measured at low stack frequency  $R_{pol}$  is shown in Fig. 14. It gradually, increasing according to time for a cathode relative humidity crescent. Because the relative humidity affects the proton mobility at high frequency.

Fig. 15 presents the arc–summit frequency behavior  $f_{max}$ . The arc–summit frequency is constant regardless of the relative humidity variation and time.

Figs. 16 and 17 shows that the arc-summit imaginary value  $I_{max}$  and the Nyquist diagram area ( $Re(Z) \cdot Im(Z)$ ), are increasing

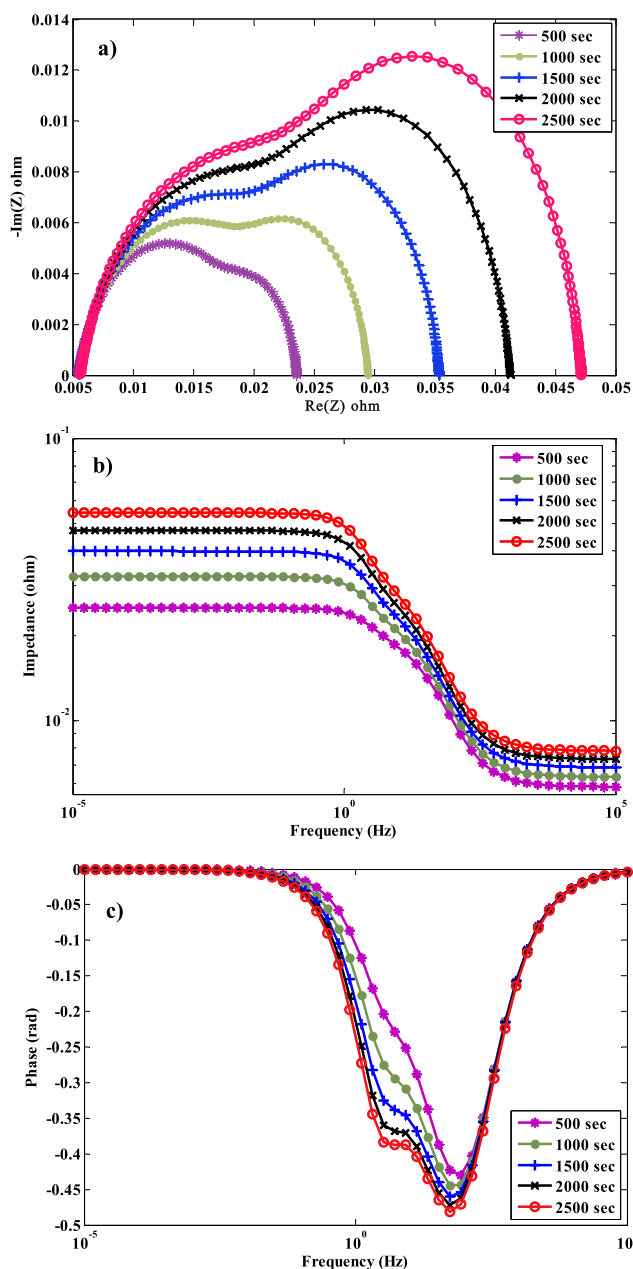


**Fig. 9 – Nyquist and Bode diagrams according to the different operating time for a dehydrating conditions of RH = 10%. a) Nyquist diagram, b), c) Bode diagram.**

with the time, when the cathode relative humidity increasing from 10% to 150%. Because the PEMFC membrane conductivity is directly related to its water content. When relative humidity increases, the water content in membrane increases, consequently the membrane conductivity increases and the stack internal resistance will decrease.

## Conclusion

In this paper, we have developed a new model for the reproduced of the Randles model with CPE, which represents the

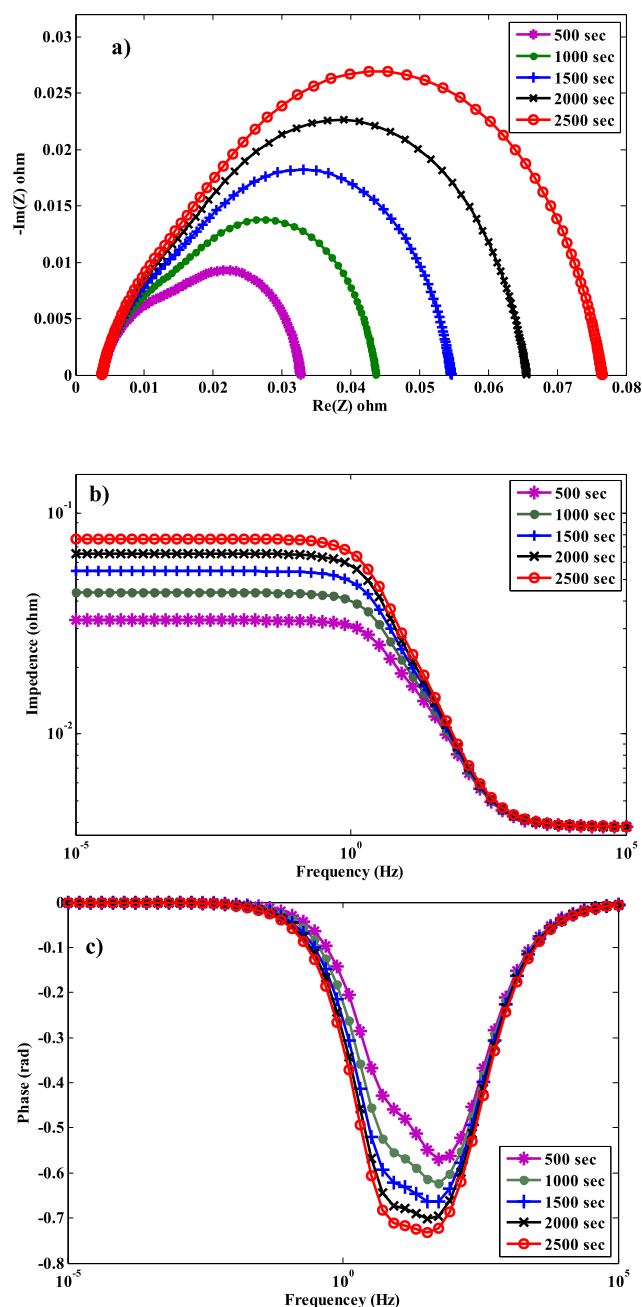


**Fig. 10 – Nyquist and Bode diagrams according to the different operating time for a flooding conditions of RH = 100%. a) Nyquist diagram, b), c) Bode diagram.**

PEM fuel cell impedance. Neural network technique (ANN) was used to create an impedance optimal model of the PEM fuel cell, for evaluating the impacts of the relative humidity and the operation time of the fuel cell impedance. This robust and reliable approach, allowed us to identify a set of two parameters (resistance measured at high frequency of the stack and the resistance measured at low frequency of the stack) which exhibiting high sensitivity to flooding or drying of the membrane-electrode assembly.

The resistance measured value at a high stack frequency  $R_{int}$  increases with time, when the cathode relative humidity

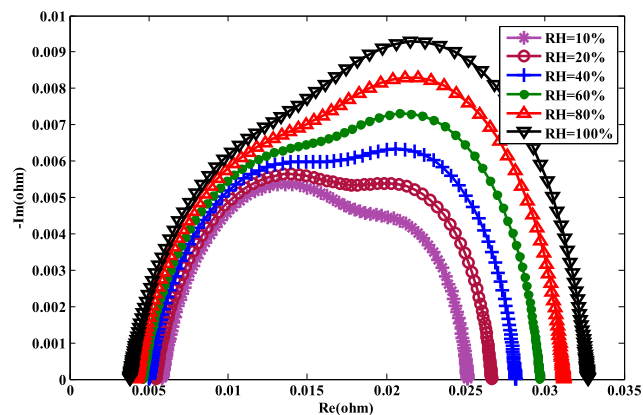


Fig. 11 – Relative humidity effect on PEMFC state at 500 s.

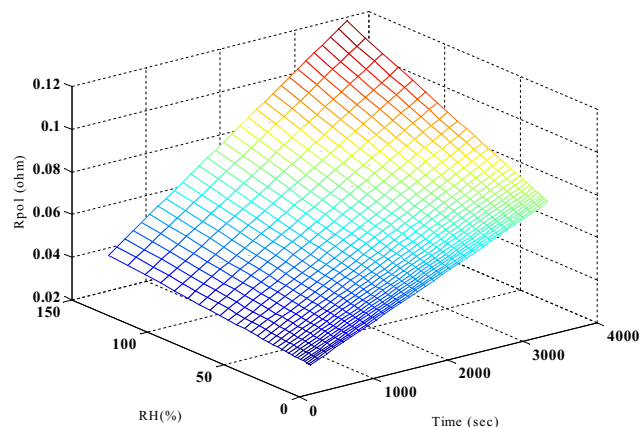


Fig. 14 – Biasing resistor.

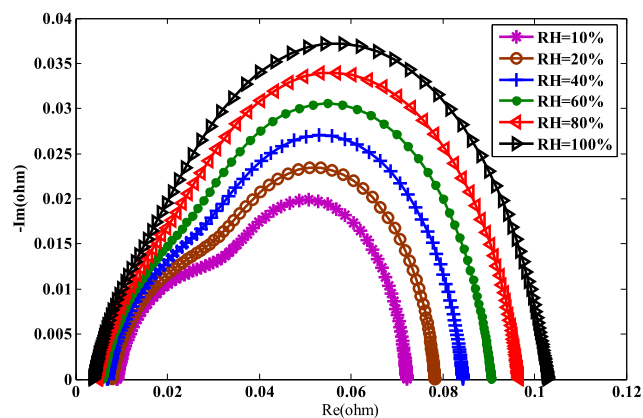


Fig. 12 – Relative humidity effect on PEMFC state at 2500 s.

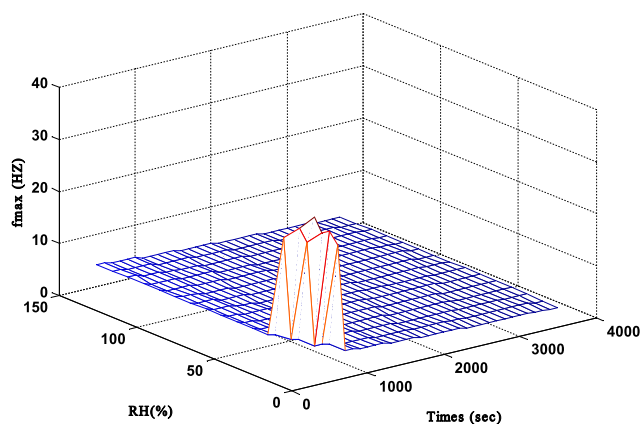


Fig. 15 – Arc-summit behavior.

decreases from 150% at 10%. The resistance measured at low stack frequency  $R_{pol}$  gradually increases, according to the time when the cathode relative humidity will increase. The arc-summit frequency behavior  $f_{max}$  is constant regardless of the relative humidity variation and time. The arc-summit imaginary value  $I_{max}$  and the Nyquist diagram area ( $Re(Z) \cdot Im(Z)$ ) are increasing with the time, when the cathode

relative humidity increasing from 10% to 150%. Because the PEMFC membrane conductivity is directly related to its water content. When relative humidity increases, the water content in membrane increases, consequently the membrane conductivity increases and the stack internal resistance will decrease.

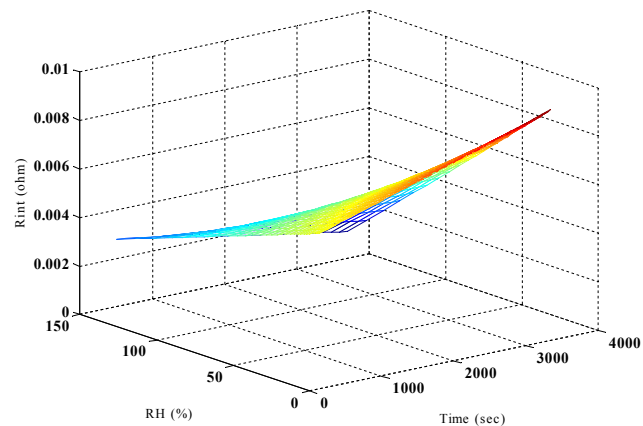


Fig. 13 – Internal resistors behavior.

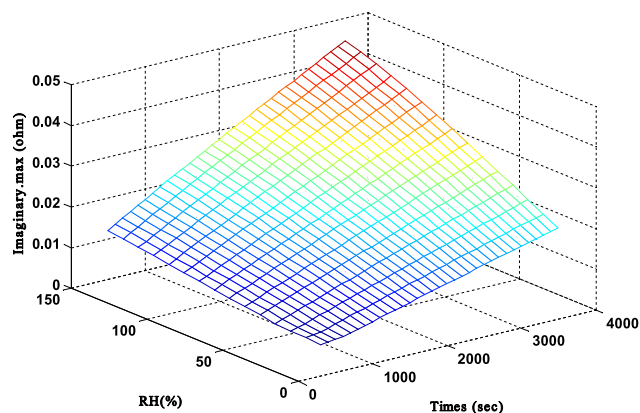


Fig. 16 – Imaginary of arc summit behavior.



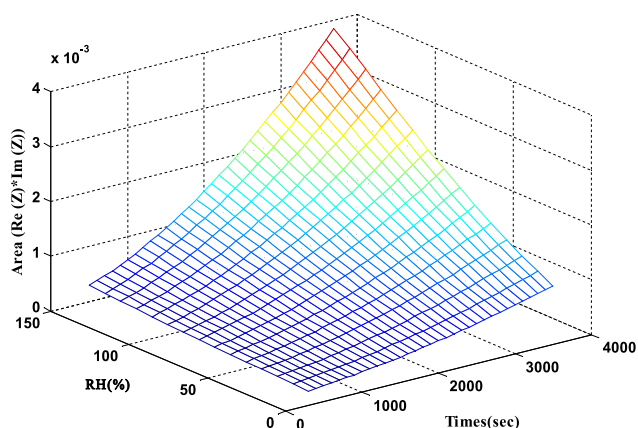


Fig. 17 – Area ( $\text{Re}(Z) \cdot \text{Im}(Z)$ ) behavior.

This model is able to easily generate Nyquist diagram for any condition of relative humidity and operating time, it helped define the stack hydration status. Based on the obtained results, the model demonstrated a best flexible response, accurate and fast. The developed model can be integrated into a water management control system in PEM fuel cells.

## REFERENCES

- [1] Corrêa JM, Farret FA, Canha LN, Simões MG. An electrochemical-based fuel-cell model suitable for electrical engineering automation approach. *IEEE T Ind Electron* 2004;51:1103–12.
- [2] Srinivasulu GN, Subrahmanyam T, Rao VD. Parametric sensitivity analysis of PEM fuel cell electrochemical Model. *Int J Hydrogen Energy* 2011;36:14838–44.
- [3] Zhiyu Y, Tao X, Zhixiang L, Yun P, Weirong C. Study on Air-cooled self-humidifying PEMFC control method based on segmented predict negative feedback control. *Electrochim Acta* 2014;132:389–96.
- [4] Fouquet N, Doulet C, Nouillant C, Dauphin-Tanguy G, Ould-Bouamama B. Model based PEM fuel cell state-of-health monitoring via ac impedance measurements. *J Power Sources* 2006;159:905–13.
- [5] Génevé T, Régnier J, Turpin C. Fuel cell flooding diagnosis based on time-constant spectrum analysis. *Int J Hydrogen Energy* 2016;41:516–23.
- [6] Mammar K, Chaker A. Flooding and drying diagnosis of proton exchange membrane fuel cells using electrochemical impedance spectroscopy analysis. *J Electr Eng* 2013;13:147–54.
- [7] Dotelli G, Ferrero R, Stampino PG, Latorrata S, Toscani S. Diagnosis of PEM fuel Cell drying and flooding based on power converter ripple. *IEEE Trans Instrum Meas* 2014;63:2341–8.
- [8] Murugesan K, Senniappan V. Investigation of water management dynamics on the performance of a Ballard-Mark-V proton exchange membrane fuel cell stack system. *Int J Electrochem Sci* 2013;8:7885–94.
- [9] Arriagada J, Olausson P, Selimovic A. Artificial neural network simulator for SOFC performance prediction. *J Power Sources* 2002;112:54–60.
- [10] Lee WY, Park GG, Yang TH, Yoon YG, Kim CS. Empirical modeling of polymer electrolyte membrane fuel cell performance using artificial neural networks. *Int J Hydrogen Energy* 2004;29:961–6.
- [11] Hatti M, Tioursi M. Dynamic neural network controller model of PEM fuel cell system. *Int J Hydrogen Energy* 2009;34:5015–21.
- [12] Chávez-Ramírez AU, Muñoz-Guerrero R, Durón-Torres SM, Ferraro M, Brunaccini G, Sergi F, et al. High power fuel cell simulator based on artificial neural network. *Int J Hydrogen Energy* 2010;35:12125–33.
- [13] Antonacci P, Chevalier S, Lee J, Yip R, Ge N, Bazylak A. Feasibility of combining electrochemical impedance spectroscopy and synchrotron X-ray radiography for determining the influence of liquid water on polymer electrolyte membrane fuel cell performance. *Int J Hydrogen Energy* 2015;40:16494–502.
- [14] Randles JEB. Kinetics of rapid electrode reactions. *Discuss Faraday Soc* 1947:1.
- [15] Rezaei Niya SM, Hoorfar M. Study of proton exchange membrane fuel cells using electrochemical impedance spectroscopy technique a review. *J Power Sources* 2013;240:281–3.
- [16] Hou Y, Zhang X, Lu X, Hao D, Ma L, Li P. AC impedance characteristics of a vehicle PEM fuel cell stack under strengthened road vibrating conditions. *Int J Hydrogen Energy* 2014;39:18362–8.
- [17] Petrone R, Zheng Z, Hissel D, Péra MC, Pianese C, Sorrentino M, et al. A review on model-based diagnosis methodologies for PEMFCs. *Int J Hydrogen Energy* 2013;38:7077–81.
- [18] Depernet D, Narjiss A, Gustin F, Hissel D, Péra MC. Integration of electrochemical impedance spectroscopy functionality in proton exchange membrane fuel cell power converter. *Int J Hydrogen Energy* 2016;41: 5378–8.
- [19] Pérez-Page M, Pérez-Herranz V. Study of the electrochemical behaviour of a 300 W PEM fuel cell stack by Electrochemical Impedance Spectroscopy. *Int J Hydrogen Energy* 2014;39:4009–15.
- [20] Wu J, Yuan XZ, Wang H, Blanco M, Martin JJ, Zhang J. Diagnostic tools in PEM fuel cell research: part I electrochemical techniques. *Int J Hydrogen Energy* 2008;33:1735–6.
- [21] Asghari S, Mokmeli A, Samavati M. Study of PEM fuel cell performance by electrochemical impedance spectroscopy. *Int J Hydrogen Energy* 2010;35:9283–90.
- [22] Mikhailenko SD, Guiver MD, Kaliaguine S. Measurements of PEM conductivity by impedance spectroscopy. *Solid State Ionics* 2008;179:619–24.
- [23] Mammar K, Chaker A. Neural Network-Based Modeling of PEM fuel cell and Controller Synthesis of a stand-alone system for residential application. *Int J Comput Sci Issues* 2012;9: 1694–4.
- [24] Demuth H, Beale M, Hagan M. *Neural Network Toolbox™ 6 User's Guide*. Version 6.0.3. COPYRIGHT 1992–2009 by The MathWorks, Inc. ISBN 0-9717321-0-8.
- [25] Fausett Laurene V. *Fundamentals of neural networks: architectures, algorithms, and applications*. Prentice-Hall international editions. Prentice-Hall; 1994. ISBN 0133341860, 9780133341867.